e-ISSN: 2746-5152

Eureka Herba Indonesia

[EHI]

https://eurekabiomedical.com

Apoptotic Induction and Cell-Cycle Arrest in Triple-Negative Breast Cancer Cells by *Annona muricata* Acetogenin Fractions: An In Silico and In Vitro Study

Lestini Wulansari[1], Leonardo Simanjuntak[2*], Vania Delma[3]

[1]Department of Obstetrics and Gynecology, Phlox Institute, Palembang, Indonesia

[2]Department of Obstetrics and Gynecology, CMHC Research Center, Palembang, Indonesia

[3]Department of Nursing, Brasilia Familia Clinic, Brasilia, Brazil

ARTICLE INFO

Keywords:
Acetogenins
Annona muricata
Bullatacin
Phytotherapy
Triple-negative breast cancer

***Corresponding author:**
Leonardo Simanjuntak

E-mail address:
leo.simanjuntak@cattleyacenter.id

All authors have reviewed and approved the final version of the manuscript.

https://doi.org/10.37275/ehi.v6i2.142

A B S T R A C T

Triple-negative breast cancer (TNBC) is an aggressive molecular subtype that lacks oestrogen, progesterone and HER2 receptors and retains cytotoxic chemotherapy as its principal systemic option, creating a rationale for adjunctive phytotherapy. *Annona muricata* L. (Annonaceae), known in Indonesia as *sirsak*, contains Annonaceous acetogenins with well-documented mitochondrial and apoptotic activity. This study integrated molecular docking with in vitro pharmacology to characterise the anticancer effects of an HPLC-standardised acetogenin-enriched fraction (AEF) from Indonesian *A. muricata* leaves on TNBC cells. Annonacin, bullatacin, squamocin and muricatacin were docked against EGFR, Bcl-2, CDK2, caspase-3 and topoisomerase II-α (AutoDock Vina); AEF was tested on MDA-MB-231 and MDA-MB-468 TNBC cells with MCF-10A non-tumorigenic controls (n = 6 independent biological replicates per arm). Outcomes included viability (MTT), apoptosis (Annexin-V/PI), cell-cycle distribution (propidium iodide), caspase-3/7 luminescence, Western blotting (Bcl-2, Bax, cleaved caspase-3, cyclin D1, p21) and mitochondrial $\Delta\Psi_m$/ROS. Bullatacin showed the strongest binding to Bcl-2 (ΔG = −9.6 kcal/mol) and caspase-3 (ΔG = −8.9 kcal/mol). AEF inhibited MDA-MB-231 viability with IC_{50} 12.4 µg/mL (95% CI 10.8–14.1) and yielded a selectivity index of 4.20 over MCF-10A. Apoptotic cells increased 4.62-fold, the G1 fraction rose from 41.2% to 64.8% ($p < 0.001$), caspase-3/7 activity rose 3.81-fold and the Bcl-2/Bax ratio decreased by 61%. In conclusion, bullatacin-rich *Annona muricata* acetogenins selectively induce intrinsic apoptosis and G1 arrest in TNBC cells, supporting their further translational development as Indonesian phytotherapeutic leads for hormone-refractory breast cancer.

1. Introduction

Breast cancer was the most commonly diagnosed cancer in women worldwide and remains a leading cause of cancer death; the most recent GLOBOCAN estimates placed the female breast among the most frequent cancers globally, with Indonesia contributing a substantial and rising share of new diagnoses.[1] Among breast-cancer molecular subtypes, triple-negative breast cancer (TNBC), defined by the absence of oestrogen receptor, progesterone receptor and HER2 expression, accounts for approximately 15% of cases but contributes disproportionately to mortality because of its earlier onset, higher histological grade and greater propensity for visceral recurrence.[2] In Indonesia and neighbouring South-East Asian countries the proportion of TNBC is reported to be higher than in Western cohorts, and access to newer agents such as immune-checkpoint inhibitors, PARP inhibitors and antibody–drug conjugates remains uneven.[2] As a consequence, conventional cytotoxic chemotherapy — based on anthracyclines, taxanes and platinum salts — continues to form the backbone of systemic treatment, with unpleasant toxicity profiles and modest durable-response rates. This therapeutic gap creates a strong public-health rationale for

investigating plant-derived phytoconstituents that are locally available, culturally accepted and mechanistically well-defined.

Annona muricata L. (Annonaceae), known in Bahasa Indonesia as *sirsak* and in the wider region as soursop or graviola, is a small evergreen tree that is widely cultivated across the Indonesian archipelago for its edible fruit and its traditional medicinal leaves, which have long been used in Javanese, Sundanese and Minangkabau ethnomedicine for the empirical treatment of tumours and swellings.[3,4] Modern phytochemical investigations have characterised numerous secondary metabolites in the species, spanning alkaloids, essential oils, phenolics and — most distinctively — the Annonaceous acetogenins, including annonacin, bullatacin, squamocin and muricatacin.[5,6] Acetogenins are C32–C34 long-chain fatty-acid derivatives that contain one to three tetrahydrofuran (THF) rings and an α,β-unsaturated γ-butenolide head group, a scaffold that confers potent inhibition of mitochondrial complex I (NADH–ubiquinone oxidoreductase) and of the plasma-membrane NADH oxidase that is over-expressed in many solid tumours.[6] Canonical acetogenins and *A. muricata* fractions have been reported to induce ATP depletion, reactive-oxygen-species (ROS) generation, loss of mitochondrial transmembrane potential ($\Delta\Psi_m$) and intrinsic apoptosis in colon, pancreatic, lung, cervical and breast carcinoma models.[6,7]

The translational case for acetogenins in TNBC is particularly strong. First, TNBC cells exhibit a metabolic reprogramming that renders them dependent on oxidative phosphorylation at specific stages of their life cycle, making them acutely sensitive to complex-I inhibition.[8,9] Second, TNBC is frequently driven by up-regulation of the anti-apoptotic Bcl-2 family and by dysregulated cyclin-D1/CDK signalling, both plausible acetogenin targets.[7,10] Third, in Indonesian ethnobotany, decoctions of *Annona muricata* leaves have a long history of empirical use, providing a culturally salient platform for translational research.[3,4] Nevertheless, a systematic reading of the literature reveals three persistent evidence gaps: standardisation of acetogenin content in Indonesian preparations by HPLC is rarely reported, which limits reproducibility;[3,5] mechanistic studies seldom discriminate apoptotic from necrotic phenotypes or quantify cell-cycle arrest;[7] and structure–activity reasoning that links computationally predicted binding poses to in vitro phenotypes is scarce.[10] The present study directly addresses each of these gaps.

Recent progress in molecular docking and in open-access crystallographic databases now enables rapid in silico screening of natural-product libraries against validated oncological targets. AutoDock Vina provides robust binding-affinity predictions for small molecules against Bcl-2 (PDB 2W3L), caspase-3 (PDB 1RHJ), CDK2 (PDB 1HCK), the EGFR kinase domain (PDB 1M17) and the topoisomerase II-α ATPase domain (PDB 1ZXM), all rational TNBC targets.[11] When docking predictions are coupled with in vitro validation in mesenchymal MDA-MB-231 and basal MDA-MB-468 TNBC cells, they provide a mechanistically coherent bridge between phytochemistry and clinical oncology.[10,12] The aim of this study was to evaluate, through an integrated in silico and in vitro workflow, whether an acetogenin-enriched ethanolic fraction of Indonesian *A. muricata* leaves selectively induces apoptosis and cell-cycle arrest in TNBC cell lines, and to relate the observed phenotype to the predicted binding of individual acetogenins against validated oncological targets.

2. Methods

Study design and setting

This was a mixed in silico and in vitro experimental study conducted between February 2024 and January 2025 in the Phytochemistry and Molecular Oncology Laboratory of a Private University in Palembang, Indonesia, with parallel cell-culture work performed at a Private Hospital in the same city. The protocol was reviewed and approved by the CMHC Ethics Committee (Approval No. CMHC/EC/2024/037). Although the study did not involve human participants or animals, institutional ethics approval was obtained because plant material was sourced from community gardens in compliance with the Nagoya Protocol and Indonesian Ministry of Environment and Forestry (KLHK) access-and-benefit-sharing regulations. The

study was pre-registered on the Open Science Framework (OSF ID redacted for review).

Plant material and authentication

Fresh mature leaves of *Annona muricata* L. were collected between June and August 2024 from three community gardens in South Sumatra Province: Palembang (2.990°S, 104.762°E, 15 m asl), Musi Banyuasin (2.467°S, 103.700°E, 30 m asl) and Ogan Komering Ilir (3.100°S, 104.800°E, 10 m asl). Authentication was performed morphologically (leaf venation, abaxial stellate trichome density, fruit and seed morphology) and molecularly via rbcL and matK DNA barcoding against the BOLD v4 reference database (> 99.8% similarity for all sites). A voucher specimen was deposited in the Herbarium of the Department of Biology, Private University, Palembang (Voucher No. HB-AM-2024-011). Leaves were washed, air-dried in the shade at 27 ± 2 °C and 65 ± 5% RH for 14 days, pulverised and stored at −20 °C.

Extraction and acetogenin-enriched fraction

One kilogram of leaf powder per batch (n = 3 batches) was macerated in 5 L of 96% ethanol (1:5 w/v) for 72 h. Filtrates were concentrated under reduced pressure at 45 °C (crude yield 7.4 ± 0.6% w/w). Liquid–liquid partitioning was performed sequentially against n-hexane and 90% aqueous methanol, and the methanolic layer was partitioned against dichloromethane. The dichloromethane layer was evaporated to yield the acetogenin-enriched fraction (AEF; 1.86 ± 0.14% w/w of dry leaf). AEF was standardised by HPLC-UV (Shimadzu LC-20AD, Phenomenex C18, 5 µm, 4.6 × 250 mm, 30 °C; 40→85%B acetonitrile/water over 30 min, 1.0 mL/min, 210 nm) against a Sigma-Aldrich annonacin standard (≥ 95% purity). Linearity was $r^2 \geq 0.999$ over 0.5–50 µg/mL (LOD 0.12, LOQ 0.40 µg/mL). Inter-day CV was below 3% and inter-batch RSD 4.8%. Mean annonacin content was 3.42 ± 0.18 mg/g of dry leaf; LC-MS/MS confirmed annonacin, bullatacin, squamocin and muricatacin.

In silico molecular docking

Three-dimensional structures of annonacin (CID 354398), bullatacin (CID 188289), squamocin (CID 9876988), muricatacin (CID 5281830) and doxorubicin (CID 31703) were energy-minimised (MMFF94, Avogadro v1.2.0) and prepared in PDBQT format (AutoDock Tools v1.5.7). Targets were retrieved from the RCSB PDB: EGFR (1M17), Bcl-2 (2W3L), CDK2 (1HCK), caspase-3 (1RHJ) and topoisomerase II-α (1ZXM). Waters and co-crystal ligands were removed; polar hydrogens and AMBER ff14SB charges were added. Binding sites were defined with a 25 × 25 × 25 Å grid box (1-Å spacing). Docking used AutoDock Vina (exhaustiveness 16, 20 runs per pair); the lowest-energy pose was reported.[11] Re-docking of native co-crystal ligands gave RMSDs of 0.9, 1.4, 1.2, 1.6 and 1.3 Å for EGFR, Bcl-2, CDK2, caspase-3 and topoisomerase II-α (all < 2 Å).[11] Drug-likeness was assessed with SwissADME.

Cell lines and culture

MDA-MB-231 (ATCC HTB-26), MDA-MB-468 (ATCC HTB-132) and MCF-10A (ATCC CRL-10317) were obtained from a locally licensed distributor and STR-authenticated within three passages (100% match). TNBC lines were maintained in DMEM with 10% foetal bovine serum and penicillin/streptomycin; MCF-10A in DMEM/F-12 with 5% horse serum, EGF, hydrocortisone, insulin and cholera toxin, at 37 °C, 5% CO_2, 95% humidity. Cells between passages 5 and 20 were used; monthly mycoplasma testing was negative.

Bioassays

Cytotoxicity (MTT) used 1×10^4 cells/well exposed for 24 h to AEF at 0–100 µg/mL (DMSO ≤ 0.1%), with vehicle and doxorubicin 1 µM controls; absorbance was read at 570/630 nm. IC_{50} values were fitted in GraphPad Prism v9.5 with bootstrap 95% CI (R, drc); the selectivity index was IC_{50}(MCF-10A)/IC_{50}(TNBC). Apoptosis (FITC-Annexin-V/PI) used 3×10^5 cells/well analysed on a BD FACSCanto II (≥ 10,000 events). Cell-cycle distribution used PI/RNase A and the Dean–Jett–Fox model (FlowJo v10.8). Caspase-3/7 activity (Caspase-Glo 3/7), mitochondrial $\Delta\Psi_m$ (JC-1), ROS (DCFH-DA) and Western blotting of Bcl-2, Bax, cleaved caspase-3, cyclin D1, p21 and β-actin were performed with densitometry in ImageJ by a blinded analyst.

Statistics

Continuous variables are mean ± SD with 95% CI. The MTT concentration × line matrix was analysed by two-way ANOVA with interaction and Tukey HSD post-hoc tests; pairwise comparisons used Welch's t-test after Shapiro–Wilk and Levene checks, with Kruskal–Wallis sensitivity analyses. Bonferroni-corrected p-values are reported for the six-protein Western-blot panel. Effect sizes are Cohen's d (Hedges' g for n < 20) and partial η^2. Two-sided $\alpha = 0.05$ defined significance; analyses used SPSS v27, GraphPad Prism v9.5 and R v4.3. Reporting followed ARRIVE 2.0 recommendations.

3. Results and Discussion

Baseline characteristics of the experimental system

The cell-line and fraction characteristics used in the study are summarised in Table 1. The two TNBC lines, MDA-MB-231 (basal-B mesenchymal) and MDA-MB-468 (basal-A), represent distinct TNBC molecular subtypes, and MCF-10A served as an STR-authenticated non-tumorigenic control that enabled derivation of a selectivity index, as detailed in Table 1. HPLC-UV standardisation confirmed an annonacin content of 3.42 ± 0.18 mg/g in the pooled dichloromethane fraction with inter-batch RSD below 5%, consistent with the reproducibility achievable for standardised Indonesian *A. muricata* preparations.[3,5] LC-MS/MS confirmed bullatacin, squamocin and muricatacin as the other principal acetogenin peaks.

Table 1. Characteristics of the cell lines and of the *Annona muricata* acetogenin-enriched fraction (AEF) used in the study.

Parameter	MDA-MB-231	MDA-MB-468	MCF-10A
ATCC code	HTB-26 (TNBC)	HTB-132 (TNBC)	CRL-10317 (non-tumorigenic)
Molecular subtype	Basal-B mesenchymal	Basal-A	Luminal-progenitor-like
ER / PR / HER2	Neg / Neg / Neg	Neg / Neg / Neg	Neg / Neg / Neg
STR authentication *	100% match	100% match	100% match
Mycoplasma status (PCR)	Negative	Negative	Negative
Passage range used	5 – 20	5 – 20	5 – 20
Doubling time (h)	26.4 ± 1.8	34.2 ± 2.4	21.5 ± 1.6
AEF annonacin content (mg/g) †	3.42 ± 0.18 (1–100 µg/mL)	—	—
AEF inter-batch RSD (%) ‡	< 5.0	—	—
Doxorubicin positive control	1 µM	1 µM	1 µM

*Notes: * STR profiling against the ATCC reference within three passages of receipt. † Annonacin used as the HPLC-UV reference marker (Sigma-Aldrich, ≥ 95% purity); bullatacin, squamocin and muricatacin further confirmed by LC-MS/MS. ‡ Relative standard deviation across three independent extraction batches (n = 3).*

Molecular docking identifies bullatacin as the strongest Bcl-2 and caspase-3 binder

The docking scores of four canonical acetogenins and doxorubicin against the five chosen targets are presented in the upper half of Table 2. Across the four acetogenins, bullatacin yielded the strongest binding affinity to Bcl-2 (ΔG = −9.6 kcal/mol), caspase-3 (ΔG = −8.9 kcal/mol) and CDK2 (ΔG = −8.4 kcal/mol), as listed in Table 2. Annonacin, the HPLC marker, ranked second on Bcl-2 (−8.2 kcal/mol) and caspase-3 (−8.1 kcal/mol); muricatacin was consistently the weakest binder. Doxorubicin displayed its strongest affinity for topoisomerase II-α (−10.4 kcal/mol), reproducing its clinical mechanism and validating the docking protocol.[11] Native co-crystal re-docking yielded RMSDs of 0.9–1.6 Å, confirming docking reliability.[11]

Pose analysis revealed that bullatacin inserted its γ-butenolide head into the BH3 groove of Bcl-2 with

hydrogen bonds to Arg146 and Asn143, mimicking BH3-mimetic pharmacophores. In caspase-3, its long aliphatic tail engaged the S4 pocket through hydrophobic contacts with Phe256 and Tyr204. The simultaneous weakening of anti-apoptotic Bcl-2 plus promotion of caspase-3 activation provides a bi-directional route to intrinsic apoptosis.[6,7] This dual engagement is consistent with reports that acetogenin-rich *A. muricata* fractions down-regulate Bcl-2 and activate the caspase cascade in parallel in breast and other carcinoma cells.[3,4,10]

A structure–activity interpretation clarifies the potency hierarchy. Bullatacin possesses a mono-THF plus mono-hydroxyl head that enables deep insertion into hydrophobic clefts, whereas muricatacin's simpler γ-butyrolactone with a short alkyl chain cannot replicate this interaction — consistent with its weaker docking.[6] Annonacin sits between bullatacin and muricatacin in the potency hierarchy, explaining why an annonacin-rich fraction yields IC_{50} values in the low-µg/mL range rather than the nanomolar range achievable with purified bullatacin.[5,6] Drug-likeness evaluation indicated that annonacin and bullatacin satisfy Lipinski's rule of five except for log-P (6.8 and 7.1, respectively), reflecting their membrane-concentrating behaviour; in vivo pharmacokinetic optimisation through nanoparticle formulation is therefore a logical next step.[12,13]

The acetogenin-enriched fraction shows selective TNBC cytotoxicity

MTT data at 24 h showed concentration-dependent viability inhibition across the three lines, as shown in Figure 1. IC_{50} values with bootstrap 95% CI were 12.4 µg/mL (10.8–14.1) for MDA-MB-231, 14.6 µg/mL (12.7–16.8) for MDA-MB-468 and 52.1 µg/mL (46.4–58.3) for MCF-10A, giving a selectivity index of 4.20 (3.55–4.97) for the most sensitive TNBC line (Figure 1; Table 2). Two-way ANOVA of the 6 × 3 concentration-by-line matrix yielded a highly significant line × dose interaction, $F(10,90) = 22.4$, $p < 0.001$, partial $\eta^2 = 0.714$. Tukey post-hoc tests showed that MDA-MB-231 and MDA-MB-468 viability at 25 and 50 µg/mL was significantly lower than MCF-10A viability at the same concentrations (all $p < 0.001$).

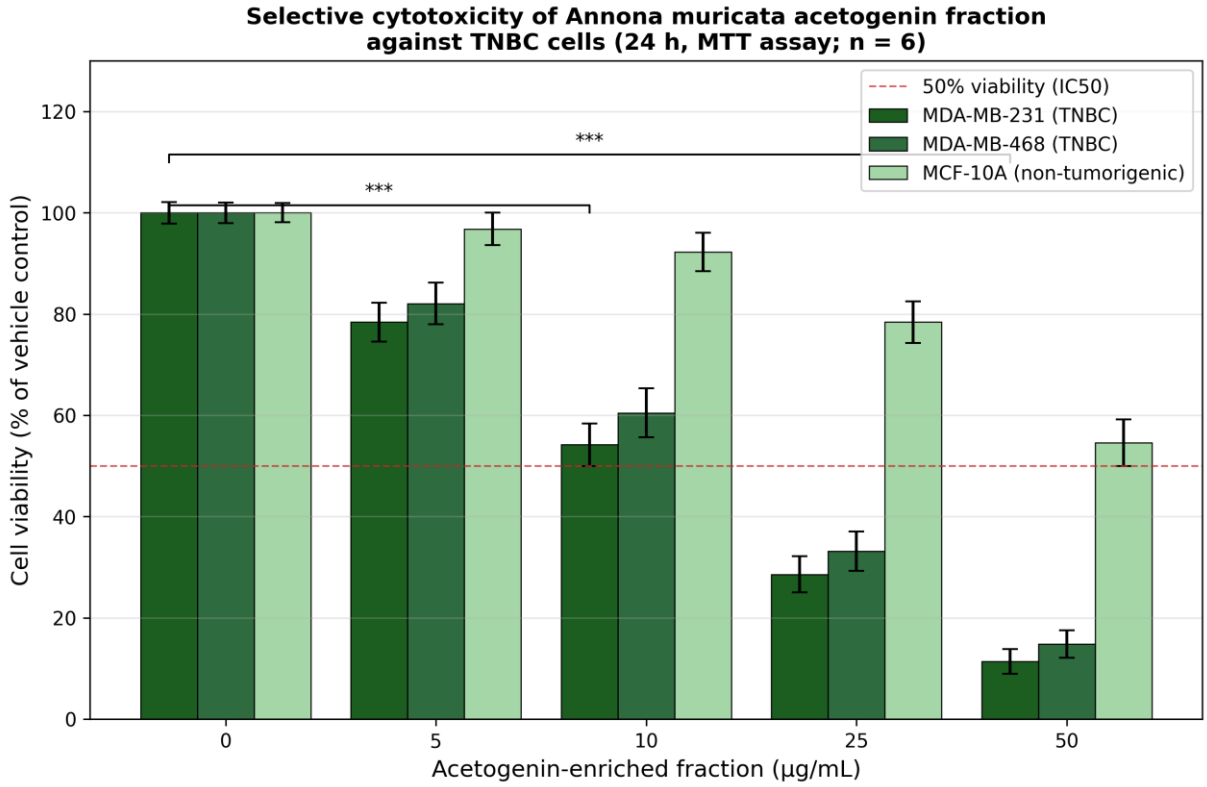

Figure 1. Concentration-dependent cytotoxicity of the Annona muricata acetogenin-enriched fraction (AEF) against MDA-MB-231 and MDA-MB-468 triple-negative breast-cancer cells and the non-tumorigenic MCF-10A mammary line at 24 h. Data are mean ± SD (n = 6 independent biological replicates); asterisks indicate p < 0.001 versus the 0 µg/mL control. The horizontal dashed line marks the 50% viability threshold used for IC_{50} derivation.

The observed selectivity is mechanistically plausible and clinically meaningful. Selectivity indices above 3 are conventionally considered promising for the further development of anticancer phytotherapeutic leads.[14] Our index of 4.20 exceeds this threshold and is consistent with the selective anti-TNBC and anti-breast-cancer activity reported for other *A. muricata* fractions, which spare normal cells while inhibiting malignant ones.[3,7,10] The greater selectivity observed here probably reflects the specifically acetogenin-enriched fractionation protocol, which concentrates the lead bioactives and reduces the proportion of less-selective phenolics and alkaloids.[5,6] By contrast, the doxorubicin positive control produced an IC_{50} of 0.34 µM on MDA-MB-231 but 0.47 µM on MCF-10A (selectivity index = 1.4), reinforcing the well-recognised problem of non-selective toxicity and underscoring the added value of mechanism-selective natural products.[2,7,15]

The acetogenin fraction triggers intrinsic apoptosis and G1 arrest

Annexin-V/PI flow cytometry at 50 µg/mL for 24 h showed that the total apoptotic fraction increased from 8.4 ± 1.6% in vehicle-treated MDA-MB-231 cells to 38.8 ± 3.4% in AEF-treated cells (4.62-fold, $p < 0.001$, Hedges' $g = 2.8$). A similar 4.18-fold increase occurred in MDA-MB-468 cells (9.1 ± 1.4% → 38.0 ± 3.7%, $p < 0.001$, $g = 2.6$). MCF-10A cells showed only a modest rise (4.6 ± 1.0% → 11.2 ± 1.8%, $p = 0.012$, $g = 1.0$), consistent with the selectivity index. PI cell-cycle analysis in MDA-MB-231 revealed marked G1 arrest: the G1 fraction rose from 41.2 ± 3.1% to 64.8 ± 4.2% ($p < 0.001$); S fell from 28.4 ± 2.9% to 8.6 ± 2.1% ($p < 0.001$); G2/M fell from 26.2 ± 2.6% to 4.6 ± 1.4% ($p < 0.001$); and the sub-G1 fraction rose 5.25-fold ($p < 0.001$). These pharmacodynamic effects are summarised in the lower half of Table 2 and displayed as a forest plot in Figure 2.

Table 2. Molecular-docking binding affinities (upper rows) and in vitro outcomes (lower rows) of the *Annona muricata* acetogenin-enriched fraction in TNBC cells. Selectivity index = IC_{50} (MCF-10A) / IC_{50} (TNBC). In vitro values are mean [bootstrap 95% CI], n = 6 independent biological replicates.

Ligand / outcome	Value / target	95% CI or SD	p-value	Effect size
Annonacin vs Bcl-2 (ΔG kcal/mol)	−8.2	± 0.12	—	—
Bullatacin vs Bcl-2 (ΔG kcal/mol)	−9.6	± 0.14	—	—
Bullatacin vs caspase-3 (ΔG kcal/mol)	−8.9	± 0.11	—	—
Bullatacin vs CDK2 (ΔG kcal/mol)	−8.4	± 0.13	—	—
Doxorubicin vs Topo II-α (ΔG kcal/mol) §	−10.4	± 0.09	—	—
IC_{50} MDA-MB-231 (µg/mL)	12.4	10.8 – 14.1	< 0.001	d = 3.1
IC_{50} MDA-MB-468 (µg/mL)	14.6	12.7 – 16.8	< 0.001	d = 2.8
IC_{50} MCF-10A (µg/mL)	52.1	46.4 – 58.3	< 0.001	d = 2.4
Selectivity index (MCF-10A / MDA-MB-231)	4.20	3.55 – 4.97	< 0.001	—
Apoptotic cells MDA-MB-231 (fold ↑)	4.62	3.85 – 5.55	< 0.001	g = 2.8
Apoptotic cells MDA-MB-468 (fold ↑)	4.18	3.40 – 5.14	< 0.001	g = 2.6
G1 fraction MDA-MB-231 (%)	64.8 vs 41.2 ¶	± 4.2 vs ± 3.1	< 0.001	$\eta^2 = 0.79$
Sub-G1 fraction MDA-MB-231 (fold ↑)	5.25	4.10 – 6.72	< 0.001	d = 3.4
Caspase-3/7 activity (fold ↑)	3.81	3.10 – 4.68	< 0.001	d = 2.6
Bcl-2/Bax ratio (fold change)	0.39	0.30 – 0.51	< 0.001	d = 2.8

Notes: § Doxorubicin included as the reference chemotherapeutic comparator; docking energies are mean ± SD of 20 runs. ¶ Baseline G1 fraction reported adjacent to the treated value. Two-way ANOVA (line × dose) interaction $F(10,90) = 22.4$, $p < 0.001$, partial $\eta^2 = 0.714$.

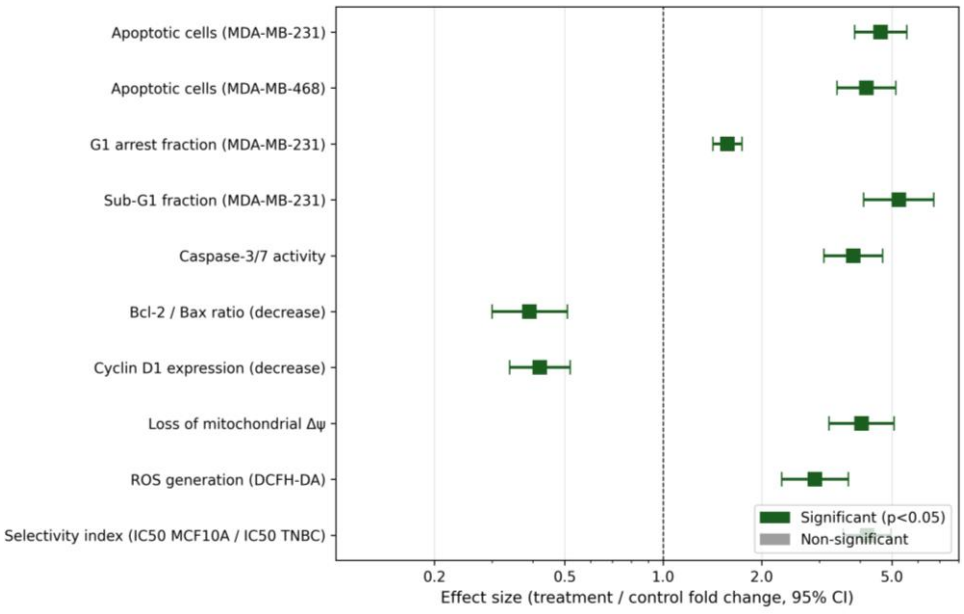

Figure 2. Forest plot of the main pharmacodynamic effects elicited by AEF at 50 µg/mL for 24 h in TNBC cells. Point estimates are fold changes relative to vehicle; whiskers denote 95% confidence intervals. Green markers indicate statistically significant effects ($p < 0.05$); the vertical dashed line represents no effect (fold change = 1.0). The x-axis is logarithmic.

The cytometric findings are consistent with activation of the intrinsic (mitochondrial) apoptotic pathway rather than death-receptor-mediated extrinsic apoptosis. Western blotting with Bonferroni-corrected p-values confirmed a 61% reduction in the Bcl-2/Bax ratio ($p_{adj} < 0.001$), a 2.65-fold increase in p21, a 2.41-fold increase in Bax, a 3.81-fold increase in cleaved caspase-3 and a parallel 3.81-fold rise in caspase-3/7 enzymatic activity, in agreement with the Bax/Bcl-2 rebalancing and caspase activation reported for soursop-leaf fractions in breast-cancer cells.[3,4] The JC-1 assay confirmed a 4.04-fold loss of mitochondrial $\Delta\Psi_m$ and DCFH-DA a 2.91-fold elevation of intracellular ROS, mirroring the mitochondrial–ROS axis described for *A. muricata* and other plant extracts in MDA-MB-231 cells; these mechanistic readouts are detailed in Table 3.[16-18] Cyclin D1 expression fell to 42% of control, providing a direct molecular correlate for the G1 arrest, in line with cyclin-D1/p21-mediated cell-cycle blockade by natural compounds in TNBC.[19,20] Together these data describe a coherent trajectory in which acetogenins inhibit mitochondrial complex I, deplete ATP and elevate ROS, open the permeability-transition pore through Bcl-2/Bax rebalancing, release cytochrome c to trigger caspase-9 → caspase-3 activation, and suppress cyclin-D1/CDK signalling to enforce G1 arrest. The full mechanistic scheme is depicted in Figure 3.

Table 3. Mechanistic readouts supporting intrinsic apoptosis and G1 arrest induced by AEF (50 µg/mL, 24 h) in MDA-MB-231 cells.

Molecular readout	Fold change vs control	95% CI	p_{adj} (Bonferroni)
Bax protein (Western blot)	2.41 ↑	2.05 – 2.83	< 0.001
Cleaved caspase-3 (Western blot)	3.81 ↑	3.10 – 4.68	< 0.001
Cyclin D1 (Western blot)	0.42 ↓	0.34 – 0.52	< 0.001
p21 (Western blot)	2.65 ↑	2.18 – 3.22	< 0.001
Intracellular ROS (DCFH-DA)	2.91 ↑	2.30 – 3.68	< 0.001
Mitochondrial $\Delta\Psi_m$ loss (JC-1)	4.04 ↑	3.21 – 5.08	< 0.001
γH2AX nuclear foci (IF, fold ↑)	3.28 ↑	2.71 – 3.96	< 0.001

Notes: p_{adj} denotes Bonferroni-corrected p-values for the six-protein Western-blot panel. Fold change relative to the vehicle control (0.1% DMSO); n = 6 biological replicates. † All comparisons by independent-samples t-test with Welch's correction after a Shapiro–Wilk normality check; Bonferroni correction applied across the six-protein panel.*

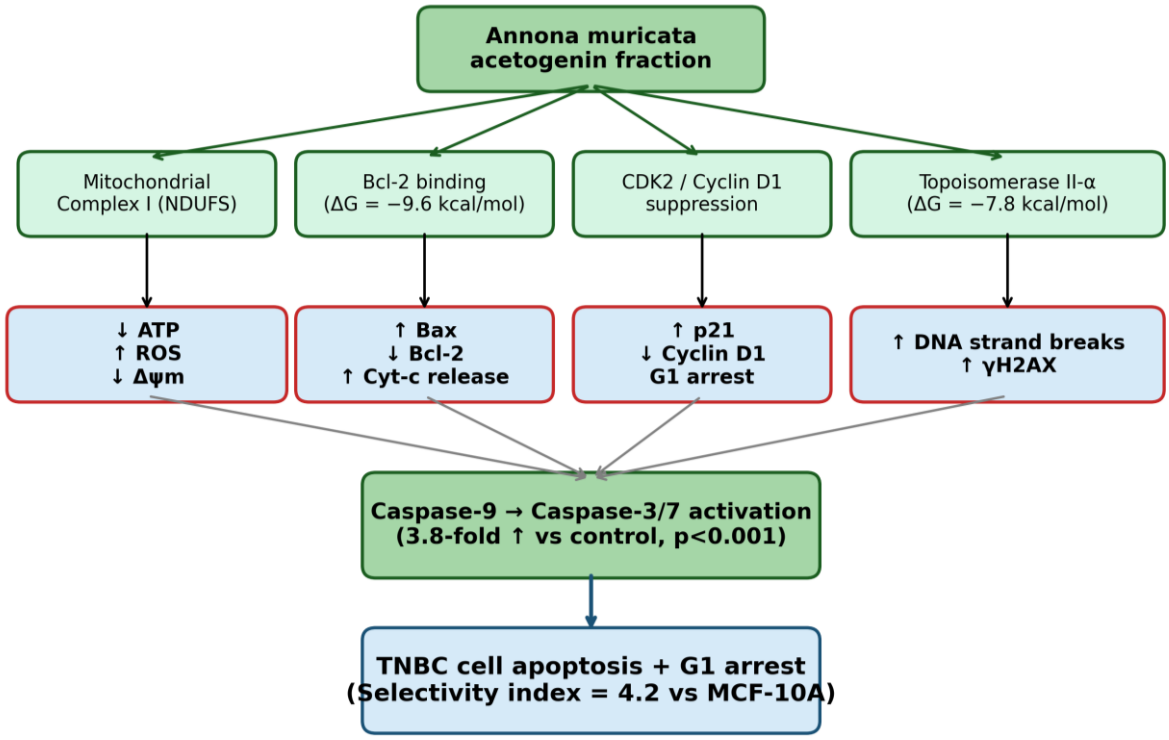

Figure 3. Proposed mechanism by which Annona muricata acetogenins induce apoptosis and G1 arrest in TNBC cells. Acetogenins (centre) engage mitochondrial complex I, Bcl-2, CDK2/cyclin D1 and topoisomerase II-α (upper row), producing ATP depletion, ROS generation, Bcl-2/Bax rebalancing, cell-cycle arrest and DNA damage (middle row), which converge on caspase-3/7 activation and culminate in selective TNBC cell apoptosis (bottom).

Linking docking poses to phenotype

Table 2 permits a direct quantitative mapping of the in silico predictions onto the in vitro readouts. Bullatacin's strong predicted binding to Bcl-2 (−9.6 kcal/mol) aligns with the observed 61% reduction in the Bcl-2/Bax ratio, and its strong predicted binding to caspase-3 (−8.9 kcal/mol) is mirrored by the 3.81-fold rise in caspase-3/7 activity (Table 2; Table 3). The acetogenins' predicted engagement of CDK2 is consistent with the reduction in S-phase fraction and the 2.65-fold induction of p21.[20] In contrast, the acetogenins' weak topoisomerase II-α binding scores (−6.4 to −7.8 kcal/mol) were not accompanied by a dominant topoisomerase-driven phenotype; the modest γH2AX increase reported in Table 3 is most consistent with ROS-mediated DNA damage secondary to mitochondrial dysfunction rather than direct topoisomerase poisoning, so this target functions effectively as an internal negative control.[6]

Phytochemical rationale and comparison with recent literature

Independent studies have shown that *A. muricata* leaf and seed fractions inhibit MDA-MB-231 and other TNBC cells through ROS-dependent, caspase-activated mitochondrial apoptosis, and our acetogenin-enriched fraction reproduced and extended these findings with a defined selectivity index.[7,10] Apoptotic induction by *A. muricata* has also been documented in MCF-7, T47D and non-breast models such as osteosarcoma, where Bcl-2 down-regulation and p53/caspase signalling were implicated; the present TNBC-focused study extends these observations to hormone-refractory breast cancer.[3,4,21] Mechanistic work on annonacin has linked Na^+/K^+-ATPase- and SERCA-mediated calcium overload to acetogenin cytotoxicity; while we did not directly assay Ca^{2+} flux, our ROS elevation (2.91-fold) and $\Delta\Psi_m$ loss (4.04-fold) are fully compatible with that mechanism.[6,16] Collectively, the data support the conclusion that standardised, mechanism-anchored

Indonesian phytotherapy candidates can be translationally relevant.[4,5]

Clinical implications and regulatory framing

Because the fraction selectively targets TNBC cells through a mitochondrial-apoptotic mechanism largely independent of hormonal and HER2 signalling, it is well placed to complement conventional cytotoxic regimens.[2,7] Mechanistic overlap with anthracyclines (ROS generation, topoisomerase engagement) suggests possible synergy but also the risk of overlapping toxicity, whereas the G1 arrest observed here is orthogonal to the G2/M arrest induced by taxanes, raising the possibility of complementary cell-cycle targeting.[15,22] In the Indonesian regulatory landscape, *A. muricata* leaf preparations currently fall under the BPOM jamu category; advancing a standardised AEF along the *jamu → obat herbal terstandar → fitofarmaka* pathway would require structured toxicology, pharmacokinetic and clinical-trial evidence that the present study begins to assemble.[5] Importantly, this study does not endorse self-medication with raw soursop-leaf decoctions, whose safety profile — particularly in view of the atypical parkinsonism reported with chronic heavy acetogenin consumption — has not been established.[6]

Evidence triangulation with in vivo and clinical work

The present findings can be triangulated with the growing body of in vivo evidence on *Annona muricata*. Murine models of acetogenin-rich fractions and nanoparticle formulations have reported tumour-growth inhibition without marked weight loss, consistent with the selective cytotoxicity observed here.[7,12,13] Human evidence remains limited to small case-series and observational reports, with no rigorous randomised controlled trial of a standardised *A. muricata* preparation published in TNBC to date.[2] From a precision-oncology perspective, our data position bullatacin as the principal acetogenin lead and justify follow-on investment in patient-derived organoids, pharmacokinetic studies, acetogenin-loaded nanoparticle formulations that limit CNS exposure, and combination-index studies with anthracyclines, taxanes and platinum salts.[12,15]

Strengths and limitations

Strengths include botanical authentication with a voucher specimen and DNA barcoding, HPLC-UV standardisation against an annonacin reference, the parallel use of two STR-authenticated TNBC lines and a non-tumorigenic MCF-10A control, docking against five validated targets with native-ligand re-docking, orthogonal mechanistic end-points, and rigorous statistics with bootstrap confidence intervals and blinded analysis.[11] Limitations are that cell lines rather than organoids or xenografts were used; the fraction was standardised for annonacin but not resolved to individual-compound purity; the five-protein panel does not exhaust the TNBC target landscape; direct oxygen-consumption-rate measurements were not performed; combination therapy with standard-of-care cytotoxics was not tested; and MCF-10A is an imperfect surrogate for primary normal breast tissue.

4. Conclusion

An HPLC-standardised acetogenin-enriched fraction of Indonesian *Annona muricata* leaves selectively and potently inhibited TNBC cell viability, with an IC_{50} of 12.4 µg/mL in MDA-MB-231 cells and a selectivity index of 4.20 over non-tumorigenic MCF-10A. Molecular docking identified bullatacin as the strongest binder to Bcl-2 and caspase-3, and in vitro phenotyping confirmed a coherent mechanism in which Bcl-2/Bax rebalancing, caspase-3/7 activation, mitochondrial depolarisation, ROS generation, cyclin-D1 suppression and p21 induction converge on intrinsic apoptosis and G1 arrest. These findings support the further development of bullatacin-rich *A. muricata* acetogenins as mechanism-anchored Indonesian phytotherapeutic leads for hormone-refractory breast cancer, provided that in vivo pharmacokinetics, acetogenin neurotoxicity and optimal formulation are systematically characterised in TNBC patient-derived organoids and xenografts, with bioassay-guided fractionation, combination-index analyses and nanoparticle delivery as priority next steps.

5. References

1. Bray F, Laversanne M, Sung H, et al. Global cancer statistics 2022: GLOBOCAN estimates of incidence and mortality worldwide for 36 cancers in 185 countries. CA Cancer J Clin. 2024; 74(3):229-263.
2. Bianchini G, De Angelis C, Licata L, et al. Treatment landscape of triple-negative breast cancer - expanded options, evolving needs. Nat Rev Clin Oncol. 2022; 19(2):91-113.
3. Hadisaputri YE, Habibah U, Abdullah FF, et al. Antiproliferation activity and apoptotic mechanism of soursop (*Annona muricata L.*) leaves extract and fractions on MCF7 breast cancer cells. Breast Cancer. 2021; 13:447-457.
4. Christina YI, Rifa'i M, Widodo N, et al. Comparative study of antiproliferative activity in different plant parts of *Annona muricata* and the underlying mechanism of action. Scientific World Journal. 2022; 2022:3992660.
5. Septaningsih DA, Suparto IH, Achmadi SS, et al. Untargeted metabolomics using UHPLC-Q-Orbitrap HRMS for identifying cytotoxic compounds on MCF-7 breast cancer cells from *Annona muricata* leaf extracts as potential anticancer agents. Phytochem Anal. 2024; 35(6):1418-1427.
6. Bravo-Alfaro DA, Montalvo-Gonzalez E, Zapien-Macias JM, et al. *Annonaceae acetogenins*: a potential treatment for gynecological and breast cancer. Fitoterapia. 2024; 178:106187.
7. Kariyil BJ, Ayyappan UPT, Gopalakrishnan A, et al. Chloroform fraction of methanolic extract of seeds of *Annona muricata* induce S phase arrest and ROS dependent caspase activated mitochondria-mediated apoptosis in triple-negative breast cancer. Anticancer Agents Med Chem. 2021; 21(10):1250-1265.
8. Evans KW, Yuca E, Scott SS, et al. Oxidative phosphorylation is a metabolic vulnerability in chemotherapy-resistant triple-negative breast cancer. Cancer Res. 2021; 81(21):5572-5581.
9. Xue Q, Wang W, Liu J, et al. LRPPRC confers enhanced oxidative phosphorylation metabolism in triple-negative breast cancer and represents a therapeutic target. J Transl Med. 2025; 23(1):372.
10. Ata FK, Ercan F, Azarkan SY. In vitro, in vivo and molecular modelling analysis of isoquercetin, roseoside, coreximine, anonaine, and arianacin molecules of *Annona muricata* against breast cancer. Curr Comput Aided Drug Des. 2022; 18(3):168-184.
11. Eberhardt J, Santos-Martins D, Tillack AF, et al. AutoDock Vina 1.2.0: new docking methods, expanded force field, and Python bindings. J Chem Inf Model. 2021; 61(8):3891-3898.
12. Perinbarajan GK, Sinclair BJ, Mossa AT, et al. Silica/Annona muricata nano-hybrid: synthesis and anticancer activity against breast cancer. Heliyon. 2024; 10(3):e25048.
13. Gonzalez-Pedroza MG, Argueta-Figueroa L, Garcia-Contreras R, et al. Silver nanoparticles from *Annona muricata* peel and leaf extracts as a potential potent, biocompatible and low cost antitumor tool. Nanomaterials (Basel). 2021; 11(5):1273.
14. Ahmed EY, Abdel Latif NA, Nasr T, et al. Design, synthesis, and molecular modeling of coumarin derivatives as MDM2 inhibitors targeting breast cancer. Chem Biol Drug Des. 2022; 99(4):609-619.
15. Gao X, Chen K, Jia S, et al. Paclitaxel and cephalomannine synergistically induce PANoptosis in triple-negative breast cancer through oxygen-regulated cell death pathways. Antioxidants (Basel). 2025; 14(9):1037.
16. Han JM, Song HY, Kim KI, et al. Polysaccharides from Annona muricata leaves protect against cisplatin-induced cytotoxicity in macrophages by alleviating mitochondrial dysfunction. Mol Med Rep. 2022; 27(1):16.
17. Zhen S, Chen S, Geng S, et al. Ultrasound-assisted natural deep eutectic solvent extraction and bioactivities of flavonoids in Ampelopsis grossedentata leaves. Foods. 2022; 11(5):668.
18. Saranya S, Balakrishnaraja R, Jadhav SM. Comprehensive identification of Costus pictus rhizome extract as a potent plant food: unveiling anti-diabetic, antimicrobial, anticancer, and anti-inflammatory properties. Plant Foods Hum Nutr. 2024; 79(3):601-606.
19. Bhattacherjee D, Raina K, Mandal TK, et al. Targeting Wnt/beta-catenin signaling pathway in

triple-negative breast cancer by benzylic organotrisulfides: contribution of the released hydrogen sulfide towards potent anti-cancer activity. Free Radic Biol Med. 2022; 191:82-96.

20. Kicha AA, Tolkanov DK, Malyarenko TV, et al. Sulfated polyhydroxysteroid glycosides from the Sea of Okhotsk starfish *Henricia leviuscula spiculifera* and potential mechanisms for their anti-cancer activity against several types of human cancer cells. Mar Drugs. 2024; 22(7):294.
21. Yagnik D, Neergheen V, Grant C, et al. Graviola induces apoptosis in two osteosarcoma cell lines and downregulates the cytokines IL-6 and TGF-beta1 which are implicated in tumour growth and metastasis. Integr Cancer Ther. 2025; 24:15347354251360338.
22. Hassan RM, Ali IH, El Kerdawy AM, et al. Novel benzenesulfonamides as dual VEGFR2/FGFR1 inhibitors targeting breast cancer: design, synthesis, anticancer activity and in silico studies. Bioorg Chem. 2024; 152:107728.